JACS
JOURNAL OF THE AMERICAN CHEMICAL SOCIETY
Communication
pubs.acs.org/JACS

NMR Solution Structure of a Photoswitchable Apoptosis Activating Bak Peptide Bound to Bcl-x_L

Piotr Wysoczanski,[†] Robert J. Mart,[†] E. Joel Loveridge,[†,#] Christopher Williams,[‡] Sara B.-M. Whittaker,[§] Matthew P. Crump,[‡] and Rudolf K. Allemann*[,†]

[†]School of Chemistry and Cardiff Catalysis Institute, Cardiff University, Main Building, Park Place, Cardiff CF10 3AT, United Kingdom

[‡]School of Chemistry, University of Bristol, Cantock's Close, Bristol BS8 1TS, United Kingdom

[§]School of Cancer Sciences, University of Birmingham, Henry Wellcome Building for Biomolecular NMR Spectroscopy, Birmingham B15 2TT, United Kingdom

Supporting Information

ABSTRACT: The Bcl-2 family of proteins includes the major regulators and effectors of the intrinsic apoptosis pathway. Cancers are frequently formed when activation of the apoptosis mechanism is compromised either by misregulated expression of prosurvival family members or, more frequently, by damage to the regulatory pathways that trigger intrinsic apoptosis. Short peptides derived from the pro-apoptotic members of the Bcl-2 family can activate mechanisms that ultimately lead to cell death. The recent development of photocontrolled peptides that are able to change their conformation and activity upon irradiation with an external light source has provided new tools to target cells for apoptosis induction with temporal and spatial control. Here, we report the first NMR solution structure of a photoswitchable peptide derived from the proapoptotic protein Bak in complex with the anti-apoptotic protein Bcl-x_L. This structure provides insight into the molecular mechanism, by which the increased affinity of such photopeptides compared to their native forms is achieved, and offers a rationale for the large differences in the binding affinities between the helical and nonhelical states.

The key regulatory protein p53 is capable of detecting genetic damage and activating the intrinsic apoptosis pathway to remove aberrant cells from the body. p53 is mutated in nearly 50% of all cancers, and in p53 wild-type cancers, it is frequently unable to perform its function due to erroneous up-regulation of its binding partners.[1] However, when disruptions of p53 signaling cause uncontrolled growth, the downstream mechanisms used to effect apoptosis may remain intact. Optically targeted activation of these pathways should lead to the selective elimination of cancer cells in an entirely natural fashion, causing minimal damage to surrounding tissues. The apoptosis effector system is largely controlled by the balance of, and interactions between, proapoptotic (e.g., Bak, Bax, tBid, Bad, Bik, NOXA) and prosurvival, that is, antiapoptotic (e.g., Bcl-x_L, Bcl-2, Mcl-1, Bcl-w) members of the Bcl-2 family of proteins.[2] When liberated from complexes with prosurvival proteins, proapoptotic Bak and Bax proteins can oligomerize in the outer mitochondrial membrane to form pores and induce the release of cytochrome c and other signaling factors.[3−5] The released proteins interact with cytosolic factors to activate the caspase cascade,[6] eventually leading to cellular engulfment by macrophages. Short peptides derived from the BH3 domains found in all Bcl-2 proteins are sufficient to bind to prosurvival Bcl-2 family members and release effector proteins from existing inert complexes.[7,8] If delivered to cells in adequate quantities, these peptides effectively stimulate the intrinsic apoptotic pathway.[9−12] Because of the entropic cost of helix formation, the α-helicity of BH3 peptides strongly correlates with their affinity for target proteins.[13−15] The recent development of photocontrolled peptides that are able to change their conformation and activity upon irradiation with external light sources offers tools to target cellular processes with temporal and spatial control.[16−23] In particular, we have shown that reversible photocontrol of the α-helicity of BH3 peptides and their affinities for target proteins can be achieved using azobenzene-derived cross-linkers,[24] thereby providing opportunities to activate apoptotic processes in cellular systems with light. Stabilization of the α-helical conformation is observed when the cross-linker is in the *cis*-configuration for peptides linked through cysteine residues in an i, $i + 7$ spacing, while the *trans*-configuration is helix-stabilizing for i, $i + 11$ spacings.[25,26] For complexes of Bcl-x_L and Bak-derived peptides, these changes in helix stabilization have been shown to be mirrored by large differences in complex stability.[24]

Here, we report the solution NMR structure of a photoswitchable, Bak derived peptide in complex with the prosurvival protein Bcl-x_L. The photoswitchable peptide used was based on the 16 residue Bak_{wt} sequence[27] with the I81F substitution (Figure 1 and Supporting Information) known to enhance the affinity for Bcl-x_L.[28] Two cysteine residues were introduced on the face of the helix anticipated to orient away from the binding region to generate the previously described $Bak_{I81F}{}^{i,i+11}$ peptide,[24] which was alkylated with 3,3′-bis(sulfo)-4,4′-bis(chloroacetamido)azobenzene (Figure S7) to produce $Bak_{I81F}{}^{i,\ i+11}$-XL.[24,26] Bcl-x_L (1−209, Δ45−84, Δ210−233)[29]

Received: March 11, 2012
Published: April 20, 2012

   dx.doi.org/10.1021/ja302390a | J. Am. Chem. Soc. 2012, 134, 7644−7647

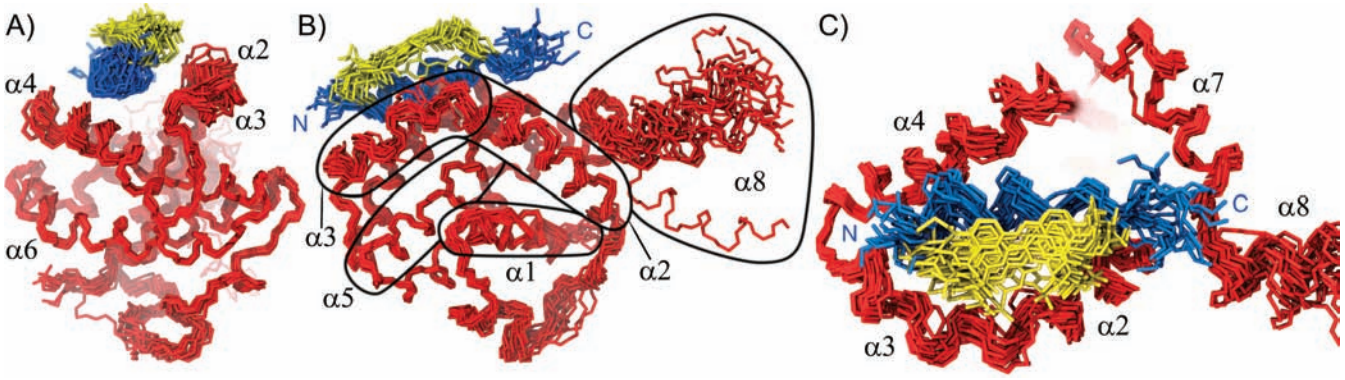

Figure 1. Three views of the NMR ensemble of Bcl-x_L (1−209, Δ45−84, Δ210−233) (red) in complex with $Bak_{I81F}^{i,i+11}$-XL ($Bak_{I81F}^{i,i+11}$: Ac-^{72}GCVGRALAAFGDCINR^{87}-NH_2) (blue). The azobenzene cross-linker is shown in yellow. Helical segments discussed in the text are labeled. The hexa-histidine affinity tag has been removed for clarity.

was produced in *E. coli* in minimal medium supplemented with U−^{13}C D-glucose and $^{15}NH_4Cl$ as sole sources of ^{13}C and ^{15}N (Supporting Information) and purified by HisTag/Ni^{2+} affinity chromatography.

A series of two- and three-dimensional NMR data sets were acquired for the chemical shift assignment and the structure determination of the complex of Bcl-x_L (1−209, Δ45−84, Δ210−233) with $Bak_{I81F}^{i,i+11}$-XL (BMRB 18238). A total of 78 unambiguous intermolecular NOEs were found, mostly between peptide residues with hydrophobic side chains and the protein (see Table S5). Restrained molecular dynamics (simulated annealing) yielded an ensemble of structures that revealed a classical Bcl-2 family member α-helical fold for Bcl-x_L (1−209, Δ45−84, Δ210−233) comprising a helix bundle organized around the core hydrophobic helix α5 (137−156, Figure 1). All nine helices, including the often truncated, flexible C-terminal α8 helix are well-defined. $Bak_{I81F}^{i,i+11}$-XL, which is coiled into a slightly distorted helix as had been suggested by previous experiments,[24] binds to the surface groove of Bcl-x_L (1−209, Δ45−84, Δ210−233) formed by helices α2 (43−100), α3 (101−112), α4 (119−129), and α5 (Figure 1C). The distortion in the α-helix of $Bak_{I81F}^{i,i+11}$-XL is centered on Cys73, one of the residues linked to the cross-linker. Val74, Leu78, Ile85 make close contacts with complementary hydrophobic patches on Bcl-x_L (1−209, Δ45−84, Δ210−233), while Phe81 points away from the bottom of the binding cleft and toward the cross-linker (Figures 2 and 3). The conformation of the cross-linker was derived by calculating structure ensembles for the four different possible conformations of the sulfonate groups (two *syn* and two *anti* configurations). Simulated annealing revealed that the *syn* arrangement, where the sulfonate groups point toward Phe81, was the lowest energy structure. Intense NOE crosspeaks between the *ortho* and *meta* protons of Phe81 (Hδ and Hε) and protons *ortho* to the sulfonates confirmed this analysis. The peptide is partially shielded from bulk solvent by the azobenzene cross-linker and both sulfonate groups point toward helices α2 and α3. Binding of $Bak_{I81F}^{i,i+11}$-XL to Bcl-x_L (1−209, Δ45−84, Δ210−233) appears to be driven almost exclusively by hydrophobic interactions. The NMR structure of uncomplexed Bcl-x_L (1−209, Δ45−84, Δ210−233) was also solved (BMRB 18250) and the rmsd between free Bcl-x_L (1−209, Δ45−84, Δ210−233) (Supporting Information) and the complex with $Bak_{I81F}^{i,i+11}$-XL was found to be 2.27 Å. As expected, the principal differences between free and complexed

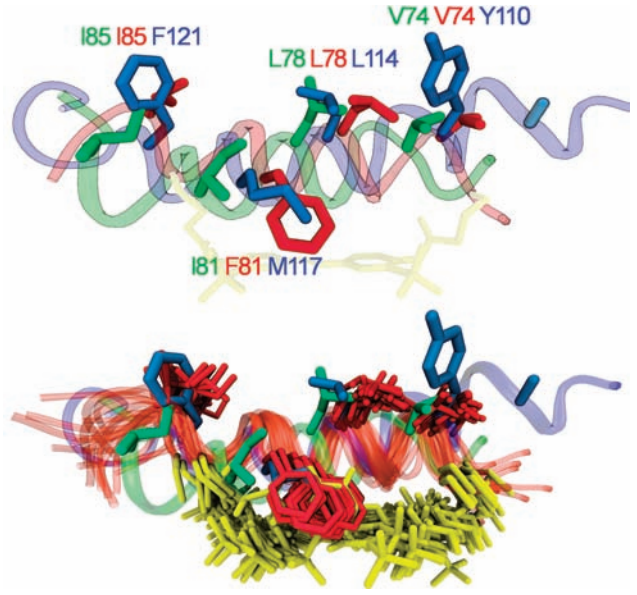

Figure 2. Overlay of the minimized average structure (top) and the complete ensemble (bottom) of conformers of $Bak_{I81F}^{i,i+11}$-XL (2LP8, red) with Bak_{wt} (1BXL, green) and Bad (1G5J, blue) peptides in the conformations found in their complexes with Bcl-x_L showing the differences in position of four hydrophobic side chains crucial for binding as well as the shift in backbone position (helical register). The side chains are viewed looking from the binding surface (Table S6 for side chain rmsd values).

Bcl-x_L (1−209, Δ45−84, Δ210−233) were found in the binding site for BH3 peptides, namely in helices α2, α3, and α4 and the loop connecting helices α3 and α4. Excluding this region (residues 94−138) from the rmsd analysis reduced the value to 0.96 Å, indicating that the remainder of the structure was largely unperturbed by ligand binding. A comparison of the structure of the complexes of Bcl-x_L (1−209, Δ45−84, Δ210−233) with $Bak_{I81F}^{i,i+11}$-XL and Bak_{wt} (1BXL)[27] revealed generally excellent agreement. The rmsd of 2.37 Å between the two structures mostly reflects differences found in three localized regions. The first is a segment from Phe105 to His113, normally designated as part of helix α3, which is disordered in the published structure of Bak_{wt}/Bcl-x_L (1−209, Δ45−84, Δ210−233) with residues occupying disallowed regions of the Ramachandran plot. In the $Bak_{I81F}^{i,i+11}$-XL/Bcl-x_L (1−209, Δ45−84, Δ210−233) complex, this area is a slightly

dx.doi.org/10.1021/ja302390a | J. Am. Chem. Soc. 2012, 134, 7644−7647

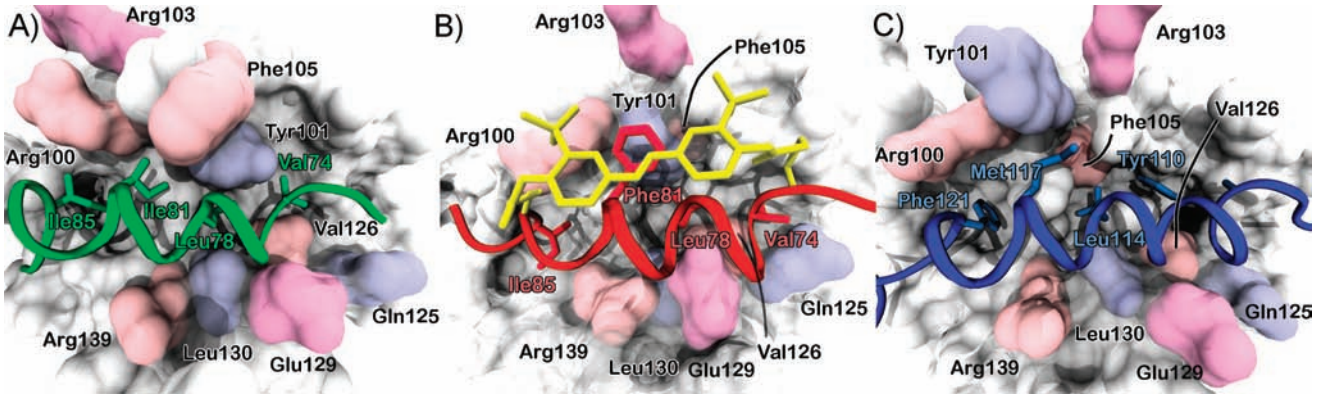

Figure 3. Comparison of the minimized average structures of (A) Bak_{wt}/Bcl-x_L (1−209, Δ45−84, Δ210−233) (1BXL), (B) $Bak_{I81F}^{i,i+11}$-XL/Bcl-x_L (1−209, Δ45−84, Δ210−233) (2LP8), and (C) Bad/Bcl-x_L (1−209, Δ49−88, Δ210−233) (1G5J).

distorted α-helix. Second, there is a smooth transition between helices α2 and α3 via a bent helix rather than the sharp turn at residue 98 previously reported for Bcl-x_L (1−209, Δ45−84, Δ210−233) bound to Bak_{wt}. Side chains of several residues in this region also undergo significant rearrangements to facilitate peptide binding. A third region of variation between the structures was found in helix α6′ (178−184) and the loop that connects helices α4 and α5. A minor shift in the side chain of Val135 of the loop causes the position of helix α3 to alter slightly to keep the side chains of Trp181 and Leu178 of the loop packed against the helix. In many respects, the structure of the complex between $Bak_{I81F}^{i,i+11}$-XL and Bcl-x_L (1−209, Δ45−84, Δ210−233) is more similar to that of Bcl-x_L bound to other BH3 peptides[30] such as Bad BH3 bound to Bcl-x_L (1−209, Δ49−88, Δ210−233) (rmsd 1.59 and 1.19 Å when residues 94−138 are not considered) (Figure 3).[13] Comparison of the conformations of $Bak_{I81F}^{i,i+11}$-XL and Bak_{wt} in the respective complexes reveals that Cys73, which is linked to the cross-linker, and the adjacent Val74 show dihedral angles that on average are slightly outside the α-helical region of the Ramachandran plot. This is probably a result of the conformational constraints imposed by the azobenzene cross-linker. In contrast to the well-defined structure in the Bak_{wt}/Bcl-x_L complex, the C-terminal asparagine and arginine residues of $Bak_{I81F}^{i,i+11}$-XL are disordered. Curiously, the $Bak_{I81F}^{i,i+11}$-XL helix is shifted by approximately 1/2 helix pitch toward the N-terminus compared to Bak_{wt} (Figure 2), similar to the position of the peptide in the Bad/Bcl-x_L (1−209, Δ49−88, Δ210−233) complex.[13] The positions of the side chains of 'hot-spot' residues of $Bak_{I81F}^{i,i+11}$-XL that make hydrophobic contacts with Bcl-x_L are also different from those observed in the Bak_{wt} complex.

Clearly, some of these distortions are imposed by the cross-linker that forces the hydrophobic side chains out of the positions adopted by the wild-type peptide. However, instead of the side chains of the peptide adjusting their position to retain optimal hydrophobic interactions, the binding site of Bcl-x_L displays a large degree of plasticity and remodels itself to make more favorable interactions with the constrained peptide (Figure 3). Such adjustments may be expected for a protein with a large number of similar but distinct binding partners.[31−34] A similar shift of α-helical register has recently been reported for the X-ray cocrystal structure of an all-hydrocarbon stapled p53 peptide and Mdm2.[27] In spite of the binding site reorganization, the affinity of the stapled peptide for Mdm2 was higher than that of a wild-type p53 peptide.[13,24,35]

The overall shape of the binding site of Bcl-x_L adapts to the presence of the cross-linker so that a more open conformation is formed, reminiscent of the structure of the Bad/Bcl-x_L complex, where Phe105 is also packed away rather than being exposed to solvent (Figure 3).[13] The ensemble of calculated structures shows that the cross-linker uses a rather limited conformational space. It is screened from the lining of the binding site on the α2/α3 helix side by Phe81, which gives strong NOE signals to protons of the aromatic rings of the cross-linker. As $Bak_{I81F}^{i,i+11}$-XL had been shown to have increased affinity for Bcl-x_L relative to the wild-type peptide, it was surprising to find that Phe81 was not inside the binding pocket but in a 'flipped out' conformation and in contact with the cross-linker. Only the Cβ-methylene group of Phe81 approaches the binding pocket where Ile81 of Bak_{wt} binds. Instead, Tyr101 rotates inward relative to its position in the Bcl-x_L/Bad complex, which slightly displaces the binding pocket for Leu78 but creates space for the cross-linker. Molecular modeling had previously suggested that a Phe81 mutation in the wild-type peptide could occupy the hydrophobic pocket of the binding site more effectively than isoleucine.[28] Subsequent fluorescence anisotropy binding measurements revealed that $Bak_{I81F}^{i,i+11}$-XL bound to Bcl-x_L (K_D = 30.5 ± 5.7 nM) with an affinity comparable to that measured for $Bak^{i,i+11}$-XL (K_D = 15.2 ± 1.3 nM). While Bak_{I81F} fits well into the binding pocket of the Bak_{wt}/Bcl-x_L structure, the presence of the azobenzene cross-linker and the remodelling of the binding site in the Bak_{I81FI}^{i+11}-XL/Bcl-x_L complex clearly favor the different conformation of Phe81.

The work presented here describes for the first time a detailed structure of an azobenzene derived photocontrolled peptide bound to its target. The NMR solution structure of the complex of $Bak_{I81F}^{i,i+11}$-XL and Bcl-x_L indicates that, while the azobenzene-stapled peptide bound to the canonical binding site, a remodelling of the binding site occurred that led to a shift in α-helical register and a perturbation of the complex structure of $Bak_{I81F}^{i,i+11}$-XL relative to that observed with the wild-type peptide. The increased affinity of such photopeptides in their α-helical conformation is clearly not just a consequence of preorganization induced by the cross-linker, but also of the formation of different hydrophobic contacts by the relocation of Phe81 between the cross-linker and the binding site on the surface of Bcl-x_L. It is likely that the light activated, non-α-helical form of the peptide cannot make these interactions,

dx.doi.org/10.1021/ja302390a | J. Am. Chem. Soc. 2012, 134, 7644−7647

which together with the cross-linker-induced destabilization of the helix may explain the large difference in the binding affinities between the helical and nonhelical states.

■ ASSOCIATED CONTENT

Supporting Information

Protocols for protein and peptide synthesis and purification, NMR sample preparation, NMR statistics and methodology, structural details of unbound Bcl-x_L and additional structural details of $Bak_{I81F}^{i,i+11}$-XL/Bcl-x_L. This material is available free of charge via the Internet at http://pubs.acs.org.

■ AUTHOR INFORMATION

Corresponding Author

allemannrk@cardiff.ac.uk

Present Address

[#]Institute of Life Sciences, Swansea University, Singleton Park, Swansea, SA2 8PP, United Kingdom.

Notes

The authors declare no competing financial interest.

■ ACKNOWLEDGMENTS

The UK's Engineering and Physical Sciences Research Council (EPSRC) supported this work through the award of Basic Technology Grant EP/F040954 (R.K.A., R.J.M., E.J.L.). The Wellcome Trust provided an equipment grant for the Bristol 600 MHz cryo-probe (WT082352). We acknowledge Marc van der Kamp for help with the parameterization of the azobenzene cross-linker.

■ REFERENCES

(1) Vousden, K. H.; Lane, D. P. *Nat. Rev. Mol. Cell Biol.* **2007**, *8*, 275.
(2) Billen, L. P.; Shamas-Din, A.; Andrews, D. W. *Oncogene* **2008**, *27* (Suppl.1), S93.
(3) Qian, S.; Wang, W.; Yang, L.; Huang, H. W. *Proc. Natl. Acad. Sci. U.S.A.* **2008**, *105*, 17379.
(4) Terrones, O.; Antonsson, B.; Yamaguchi, H.; Wang, H. G.; Liu, J.; Lee, R. M.; Herrmann, A.; Basanez, G. *J. Biol. Chem.* **2004**, *279*, 30081.
(5) Bleicken, S.; Classen, M.; Padmavathi, P. V.; Ishikawa, T.; Zeth, K.; Steinhoff, H. J.; Bordignon, E. *J. Mol. Biol.* **2010**, *285*, 6636.
(6) Shamas-Din, A.; Brahmbhatt, H.; Leber, B.; Andrews, D. W. *Biochim. Biophys. Acta* **2011**, *1813*, 508.
(7) Chittenden, T.; Flemington, C.; Houghton, A. B.; Ebb, R. G.; Gallo, G. J.; Elangovan, B.; Chinnadurai, G.; Lutz, R. J. *EMBO J.* **1995**, *14*, 5589.
(8) Zha, H.; Aime-Sempe, C.; Sato, T.; Reed, J. C. *J. Biol. Chem.* **1996**, *271*, 7440.
(9) Holinger, E. P.; Chittenden, T.; Lutz, R. J. *J. Biol. Chem.* **1999**, *274*, 13298.
(10) Shroff, E. H.; Snyder, C. M.; Budinger, G. R.; Jain, M.; Chew, T. L.; Khuon, S.; Perlman, H.; Chandel, N. S. *PLoS One* **2009**, *4*, e5646.
(11) Moreau, C.; Cartron, P. F.; Hunt, A.; Meflah, K.; Green, D. R.; Evan, G.; Vallette, F. M.; Juin, P. *J. Biol. Chem.* **2003**, *278*, 19426.
(12) Fricke, T.; Mart, R. J.; Watkins, C. L.; Wiltshire, M.; Errington, R. J.; Jones, A. T.; Allemann, R. K. *Bioconjugate Chem.* **2011**, *22*, 1763.
(13) Petros, A. M.; Nettesheim, D. G.; Wang, Y.; Olejniczak, E. T.; Meadows, R. P.; Mack, J.; Swift, K.; Matayoshi, E. D.; Zhang, H.; Thompson, C. B.; Fesik, S. W. *Protein Sci.* **2000**, *9*, 2528.
(14) Hinds, M. G.; Smits, C.; Fredericks-Short, R.; Risk, J. M.; Bailey, M.; Huang, D. C.; Day, C. L. *Cell Death Differ.* **2007**, *14*, 128.
(15) Lama, D.; Sankararamakrishnan, R. *J. Comput.-Aided Mol. Des.* **2011**, *25*, 413.
(16) Behrendt, R.; Schenk, M.; Musiol, H. J.; Moroder, L. *J. Pept. Sci.* **1999**, *5*, 519.
(17) Kusebauch, U.; Cadamuro, S. A.; Musiol, H. J.; Lenz, M. O.; Wachtveitl, J.; Moroder, L.; Renner, C. *Angew. Chem., Int. Ed.* **2006**, *45*, 7015.
(18) Renner, C.; Moroder, L. *ChemBioChem* **2006**, *7*, 869.
(19) Guerrero, L.; Smart, O. S.; Woolley, G. A.; Allemann, R. K. *J. Am. Chem. Soc.* **2005**, *127*, 15624.
(20) Guerrero, L.; Smart, O. S.; Weston, C. J.; Burns, D. C.; Woolley, G. A.; Allemann, R. K. *Angew. Chem., Int. Ed.* **2005**, *44*, 7778.
(21) Mart, R. J.; Wysoczański, P.; Kneissl, S.; Ricci, A.; Brancale, A.; Allemann, R. K. *ChemBioChem* **2012**, *13*, 515.
(22) Zhang, F.; Timm, K. A.; Arndt, K. M.; Woolley, G. A. *Angew. Chem., Int. Ed.* **2010**, *49*, 3943.
(23) Beharry, A. A.; Woolley, G. A. *Chem. Soc. Rev.* **2011**, *40*, 4422.
(24) Kneissl, S.; Loveridge, E. J.; Williams, C.; Crump, M. P.; Allemann, R. K. *ChemBioChem* **2008**, *9*, 3046.
(25) Kumita, J. R.; Smart, O. S.; Woolley, G. A. *Proc. Natl. Acad. Sci. U.S.A.* **2000**, *97*, 3803.
(26) Zhang, Z.; Burns, D. C.; Kumita, J. R.; Smart, O. S.; Woolley, G. A. *Bioconjugate Chem.* **2003**, *14*, 824.
(27) Sattler, M.; Liang, H.; Nettesheim, D.; Meadows, R. P.; Harlan, J. E.; Eberstadt, M.; Yoon, H. S.; Shuker, S. B.; Chang, B. S.; Minn, A. J.; Thompson, C. B.; Fesik, S. W. *Science* **1997**, *275*, 983.
(28) Chin, J. W.; Schepartz, A. *Angew. Chem., Int. Ed.* **2001**, *40*, 3806.
(29) Muchmore, S. W.; Sattler, M.; Liang, H.; Meadows, R. P.; Harlan, J. E.; Yoon, H. S.; Nettesheim, D.; Chang, B. S.; Thompson, C. B.; Wong, S. L.; Ng, S. L.; Fesik, S. W. *Nature* **1996**, *381*, 335.
(30) Liu, X.; Dai, S.; Zhu, Y.; Marrack, P.; Kappler, J. W. *Immunity* **2003**, *19*, 341.
(31) Lee, E. F.; Czabotar, P. E.; Yang, H.; Sleebs, B. E.; Lessene, G.; Colman, P. M.; Smith, B. J.; Fairlie, W. D. *J. Biol. Chem.* **2009**, *284*, 30508.
(32) Yang, C. Y.; Wang, S. *ACS Med. Chem. Lett.* **2011**, *2*, 280.
(33) Xu, H.; Ye, H.; Osman, N. E.; Sadler, K.; Won, E. Y.; Chi, S. W.; Yoon, H. S. *Biochemistry* **2009**, *48*, 12159.
(34) Bharatham, N.; Chi, S. W.; Yoon, H. S. *PLoS one* **2011**, *6*, 1.
(35) Baek, S.; Kutchukian, P. S.; Verdine, G. L.; Huber, R.; Holak, T. A.; Lee, K. W.; Popowicz, G. M. *J. Am. Chem. Soc.* **2011**, *134*, 103.